

Article

Stabilization of the Interface between a PEO-Based Lithium Solid Polymer Electrolyte and a 4-Volt Class Cathode, LiCoO₂, by the Addition of LiPF₆ as a Lithium Salt

Sou Taminato, Akino Tsuka, Kento Sobue, Daisuke Mori , Yasuo Takeda *, Osamu Yamamoto and Nobuyuki Imanishi

Graduate School of Engineering, Mie University, Tsu 514-8507, Japan; taminato@chem.mie-u.ac.jp (S.T.); 418m341@m.mie-u.ac.jp (A.T.); 419m333@m.mie-u.ac.jp (K.S.); daisuke.mori@chem.mie-u.ac.jp (D.M.); yamamoto@chem.mie-u.ac.jp (O.Y.); imanishi@chem.mie-u.ac.jp (N.I.)

* Correspondence: takeda@chem.mie-u.ac.jp

Abstract: Here, the time dependence of the interfacial resistance for Li/polyethylene oxide (PEO)-Li(CF₃SO₂)₂N (LiTFSI)-LiPF₆/LiCoO₂ cells was measured to investigate the stabilization effect of LiPF₆ on the interface between a solid polymer electrolyte (SPE) and a 4-volt class cathode, LiCoO₂. Impedance measurements under the applied potentials between 4.1 V and 4.4 V vs. Li/Li⁺ indicated that the addition of LiPF₆ to LiTFSI was effective in improving the stability at high potentials such as 4.4 V vs. Li/Li⁺. In contrast, the resistance of the non-doped PEO-LiTFSI/LiCoO₂ interface increased with time under the lower potential of 4.1 V vs. Li/Li⁺. Fairly good cycle performance was obtained for the LiPF₆-doped cell, even at a cut-off voltage of 4.5 V vs. Li/Li⁺.

Keywords: lithium solid polymer electrolyte; 4-volt class cathode; lithium polymer battery; lithium hexafluorophosphate



Citation: Taminato, S.; Tsuka, A.; Sobue, K.; Mori, D.; Takeda, Y.; Yamamoto, O.; Imanishi, N. Stabilization of the Interface between a PEO-Based Lithium Solid Polymer Electrolyte and a 4-Volt Class Cathode, LiCoO₂, by the Addition of LiPF₆ as a Lithium Salt. *Batteries* **2024**, *10*, 140. <https://doi.org/10.3390/batteries10040140>

Academic Editor: Masashi Kotobuki

Received: 22 February 2024

Revised: 11 April 2024

Accepted: 17 April 2024

Published: 19 April 2024



Copyright: © 2024 by the authors. Licensee MDPI, Basel, Switzerland. This article is an open access article distributed under the terms and conditions of the Creative Commons Attribution (CC BY) license (<https://creativecommons.org/licenses/by/4.0/>).

1. Introduction

Since polyethylene oxide (PEO)-based lithium solid polymer electrolytes (SPEs) were introduced in solid lithium batteries in the late 1970s [1,2], much research effort was devoted to the development of high-performance all-solid lithium polymer batteries from the 1980s to the 2000s. However, various issues associated with PEO-based electrolytes have held back the practical realization of all-solid lithium polymer batteries. The weak points of PEO–lithium salt complexes (PEO–LiX) are typically as follows. (1) The conductivity is low in the range of 10^{−7} to 10^{−8} S/cm at room temperature. Therefore, the cells must be operated at a temperature higher than 60 °C, where the amorphous phase in the PEO–salt complex becomes dominant, which is associated with the high lithium ion conductivity [3–5]. (2) High-voltage cathode materials such as LiCoO₂, Li(Ni,Co,Mn)O₂, and LiMn₂O₄ have low reversible capacities in SPE cells [6,7], which are assumed to be the result of the low decomposition potential (narrow electrochemical window) of polymer electrolytes compared with that of conventional liquid electrolytes [8].

However, such a solid polymer has a flexible and deformable character, which enables better mechanical and electrical contact with active electrode materials than that with inorganic solid electrolytes. In addition, the relatively good stability against Li metal [9] is advantageous compared to inorganic oxide and sulfide solid electrolytes, although the process is prone to lithium dendrite formation under high-current-cell operation [10–12]. The good compatibility with graphite as an anode [13,14] is also beneficial in comparison to other solid electrolytes.

Efforts to improve the poor low-temperature characteristics of PEO-based electrolytes have been continued by the modification of PEO-based polymers over the past two decades

(see cited reviews [15–17]); i.e., (1) the appropriate design and selection of easily dissociated lithium salts with a high lithium transference number (t_+) [18], (2) the addition of plasticizers to facilitate the segmental motion of polymer chains, (3) the dispersion of fine ceramic particles in the PEO matrix to improve the fraction of amorphous phase, and (4) the synthesis of copolymeric, cross-linked, or branched PEO-based polymers with structures suitable for the acceleration of lithium ion hopping.

Over the past decade, various reports aimed at an increase in the performance of SPEs have been published. Although there have been a fair number of reports on studies to improve the stability of so-called 4 V class cathodes and SPEs [19,20], sufficient battery properties have not been established as well as with liquid electrolytes. In many cases, 3 V class cathode materials, especially LiFePO_4 , have been selected to demonstrate good electrolyte performance in tested cells. No detailed discussions on the decomposition potential for high-voltage cathode materials have been reported.

The 4 V class cathode materials, such as LiCoO_2 , LiMn_2O_4 , $\text{Li}(\text{Ni}, \text{Co}, \text{Mn})\text{O}_2$, etc., that have been extensively used in liquid electrolyte cells have been known to show much lower reversible capacity in PEO-based electrolyte cells [6,7]. In 2001, we reported the cut-off voltage dependence on the capacity vs. cycling number for a $\text{Li}/\text{PEO}_{19}\text{-Li}(\text{CF}_3\text{SO}_2)_2\text{N}(\text{LiTFSI})\text{-10 wt\% BaTiO}_3/\text{LiNi}_{0.8}\text{Co}_{0.2}\text{O}_2$ cell [21], where the subscript 19 indicates that the molar ratio of Li salt to the oxygen in PEO ($\text{Li}/\text{O} = 1/19$). The cell capacity decreased rapidly with cycling by charging up to 4.0 V and discharging to 2.5 V. On the other hand, no significant capacity fade was observed by charging up to 3.9 V or less. Aihara et al. reported 500 charge–discharge cycles with 100% capacity retention in the operating range of 3.0–4.1 V for Li/LiCoO_2 cells with an SPE modified from PEO [22]. Judging from the reports on polymer electrolyte cells, the decomposition potential of PEO-related electrolytes can be estimated to be in the range from 3.7 V to 4.1 V [8,9].

The research group of the Central Research Institute of Electric Power Industry, Japan, succeeded in the relatively stable cycling of a Li/PEO -based SPE/ LiCoO_2 cell up to 4.6 V vs. Li/Li^+ (better cyclability was obtained at less than 4.4 V vs. Li/Li^+) by interposing Li_3PO_4 between the polymer electrolyte and LiCoO_2 [23,24]. Our group reported the cycle test of a $\text{Li}/[(\text{PEO}\text{-10 wt\% HBP})_{10}(\text{LiTFSI}\text{-10 wt\% LiPF}_6)]\text{-10 wt\% BaTiO}_3/\text{LiNi}_{0.8}\text{Co}_{0.2}\text{O}_2/\text{Al}$ cell, where HBP (hyperbranched polymer poly[bis(triethyleneglycol)benzoate] capped with an acetyl group) and BaTiO_3 were added to enhance the conductivity of the SPE. The addition of 10 wt% LiPF_6 to LiTFSI increased the cycle performance significantly. The initial cathode capacity of 150 mAh/g declined to 74 mAh/g after 410 charge–discharge cycles at 0.57 C with a cut-off voltage of 4.4–2.5 V. The capacity fade rate was ca. 0.12%/cycle [25], where the retention was less than that of a typical liquid electrolyte system but was largely superior to that of 4 V class solid lithium polymer cells with typical lithium salts such as LiClO_4 and LiTFSI . Aluminum current collectors are known to undergo serious corrosion in carbonate-based liquid electrolytes containing LiTFSI , whereas a protective film is formed on the aluminum surface when LiPF_6 and LiBF_4 are added to LiTFSI [26,27]. Inspired by these reports, the addition of LiPF_6 to the SPE was attempted and an improvement in the cell performance was obtained [25]; however, the reason for the improvement remained obscure.

In this paper, we provide a detailed examination of the effect of LiPF_6 addition on a $\text{Li}/\text{PEO}\text{-LiTFSI}/\text{LiCoO}_2$ cell. LiTFSI was used as a base lithium salt because, from the early period of study of all-solid lithium polymer batteries, $\text{PEO}\text{-LiTFSI}$ electrolyte systems have been used because of the high lithium ion conductivity due to the plasticization effect [28]. The PEO -to- LiTFSI ratio was fixed at $\text{Li}/\text{O} = 1/18$. Although SPE with a higher LiTFSI content has higher Li ion conductivity, the mechanical strength decreases due to the sticky and fluid tendency of the SPE; therefore, an appropriate composition with respect to both the conductivity and mechanical strength was determined. The potential stability of polymer electrolytes has often been estimated according to linear sweep voltammetry (LSV) or cyclic voltammetry (CV) results. However, from non-equilibrium dynamic LSV or CV methods conducted in a short measurement time, it is difficult to obtain information on long-term stability between SPEs and electrode materials. Therefore, the stability of the

SPE with the 4 V class LiCoO₂ cathode material was estimated by employing the static method; i.e., impedance measurements under various constant potentials were applied to the SPE/LiCoO₂ interface from 4.1 V to 4.4 V vs. Li/Li⁺. This method was modified from the report by Seki et al. [24,29].

2. Materials and Methods

All of the polymer electrolytes described here were prepared by the solvent casting technique with acetonitrile (AN) as a carrier solvent. High-molecular-weight (MW: 6×10^5) PEO (Aldrich Chemical, St. Louis, MO, USA) and Li salts (Li(CF₃SO₂)₂N (LiTFSI; Wako Pure Chemicals, Osaka, Japan) and LiPF₆ (Kishida Chemical, Osaka, Japan) were used as received. PEO and the lithium salts (LiTFSI and LiPF₆) were dissolved in AN with a molar ratio of Li/O = 1/18. The composition of LiPF₆ was set in LiTFSI:LiPF₆ weight ratios of 10:0, 9:1, 75:25, 50:50, 25:75, and 0:100. The polymer electrolyte solution was cast in a polytetrafluoroethylene (PTFE) dish under a dry argon atmosphere. The solvent in the slurry was evaporated slowly under a flow of nitrogen gas for 48 h at room temperature. The polymer electrolyte films were then dried at 120 °C under vacuum for 12 h. These procedures yielded homogenous membranes with an average thickness of ca. 300 μm.

The working electrode was composed of 95 wt% LiCoO₂ (Nihon Chemical, Kabupaten Bekasi, Indonesia) as an active material, 3 wt% acetylene black (AB; Wako Chemicals, Richmond, VA, USA) as a conductive additive, and 2 wt% polyvinylidene difluoride (PVdF; Kureha, Tokyo, Japan) as a binder. The viscosity of the slurry was adjusted to a toothpaste-like consistency by control of the *N*-methyl-2-pyrrolidone (NMP) content. The slurry obtained was cast on an aluminum foil (Thank-Metal Co., Hyogo, Japan), dried in air at 80 °C for 2 h, and then vacuum-dried at 120 °C for 3 h. Each electrode treated in a vacuum was transferred to an Ar gas-filled glove box and punched out into a 12 mm diameter, ca. 20 μm thick (exc. foil) electrode for cell assembly.

Pouch cells were used for electrochemical measurements. An SPE membrane was placed between two electrode sheets in a glove box, and these were inserted into the pouch-like film, overlapping the electrode leads, and then heat-sealed on three sides. The cell was then sandwiched between laminated sheets, and the four surrounding sides were heat-sealed. A small hole was drilled in one corner of the laminated cell and vacuumed to seal it. All operations were performed in a glove box.

The conductivities of the polymer electrolytes were measured using a symmetrical blocking cell, Au/PEO-LiTFSI-LiPF₆/Au, in a pouch cell using a frequency response analyzer (Solartron 1260) in the temperature range from 30 to 80 °C. An AC perturbation of 10 mV was applied in the frequency range from 1×10^6 to 0.1 Hz. The cells were initially heated at 80 °C and then cooled down to the measurement temperature to ensure good contact between the electrolyte and electrode.

The quasi-decomposition phenomenon of the polymer electrolytes was estimated from CV measurements of the cells, Li/electrolyte/Au and Li/electrolyte/Al, at 80 °C, where a potentiostat (Solartron 1287) was run for 5 cycles at a scan rate of 1 mV/s in the voltage range of 2.0–5.0 V vs. Li/Li⁺.

The cell for the electrochemical tests consisted of the Al metal sheet lead, LiCoO₂ cathode, the polymer electrolyte, and a lithium metal counter electrode with a Cu metal lead, all of which was sealed in a laminated sheet pack under vacuum. The test cell was heated at 80 °C for 20 h so that the polymer electrolyte penetrated into the LiCoO₂ electrode. The completion of penetration was confirmed by recognition of the equal first charge capacity to that of a Li/LiCoO₂ cell with a liquid electrolyte (LiPF₆/EC-DEC).

To evaluate the stability of the SPE with the LiCoO₂ cathode material under static conditions, AC impedance measurements were performed under each potential of the Li-deintercalated Li_{1-x}CoO₂ electrode by the combination of constant current–constant voltage charging processes. The cells were charged to 4.1 V, 4.2 V, 4.3 V, and 4.4 V vs. Li/Li⁺ with the voltage maintained for 2 h and then open-circuited for 2 h followed by the impedance measurements (from 1×10^6 to 0.05 Hz) using a multi-potentiostat with an impedance

analyzer (Biologic VMP3). The measurements were repeated 20 times to observe the variation in the interface resistance with time. All measurements were performed at 80 °C.

Charge–discharge tests of the cells were performed in the potential ranges of 2.5 V to each potential (4.2–4.4 V vs. Li/Li⁺) with a rate of 0.1 C at 80 °C.

3. Results

Figure 1 shows Arrhenius plots for the electrical conductivity of PEO₁₈(100-x)LiTFSI-xLiPF₆ as a function of x (wt%), where the subscript 18 indicates a PEO-to-Li salt ratio of Li/O = 1/18. The conductivity inflection around 60–50 °C reflects the transition from the crystalline to amorphous phase at the eutectic temperature [30,31]. The conductivity decreased with an increase in the LiPF₆ content, both in the high- and low-temperature region, although the decrease was stronger in the crystalline phase region. The transition temperature increased with the LiPF₆ content. (PF₆)[−] anions, which are smaller than (TFSI)[−] anions, attract Li⁺ ions more strongly to themselves, which could decrease both the volume fraction of the amorphous phase of the PEO–salt complex and the number of charge carriers due to the low degree of ion dissociation [4]. The conductivities at 80 °C ranged from 1.15 × 10^{−3} S/cm for 0% LiPF₆ to 0.58 × 10^{−3} S/cm for 100% LiPF₆, and those at 60 °C were from 0.54 × 10^{−3} S/cm for 0% LiPF₆ to 0.23 × 10^{−3} S/cm for 100% LiPF₆. The conductivities at 80 °C are considered acceptable for an SPE for battery operation; however, at the working temperature of 60 °C, the conductivities for the LiPF₆-rich region may be too low for high-rate cycle testing. Therefore, all the electrochemical measurements were performed at 80 °C.

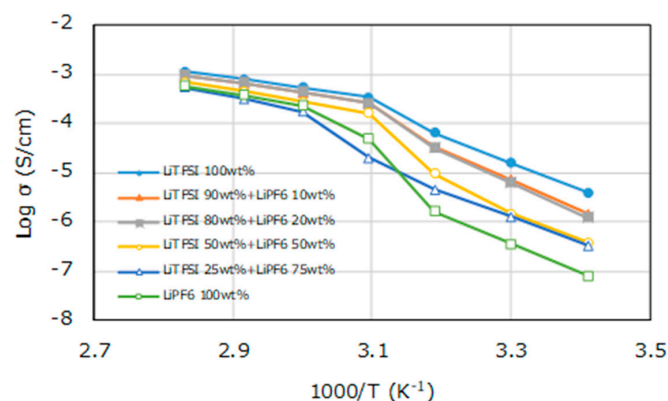


Figure 1. Temperature dependence of the electrical conductivity for PEO₁₈(100-x)LiTFSI-xLiPF₆ for various x (wt%).

At the beginning, the decomposition potentials (electrochemical stability window) and the aluminum dissolution potential of the polymer electrolytes were evaluated from CV measurements of the Li/electrolyte/Au and Li/electrolyte/Al cells. Figure 2 shows potential sweep results from 2.5 V to 5.0 V vs. Li/Li⁺ in the second cycle at 80 °C. In the first oxidation sweep, small irregular peaks appeared, which disappeared after the second cycle, and the CV curves became stable with similar curves after the second cycle. Although it is difficult to estimate the decomposition potential for each electrolyte from Figure 2a, the smaller current with a higher content of LiPF₆ indicates that the presence of LiPF₆ increases the resistance of the electrolyte against oxidative decomposition (and/or oxidative reactions with Au metal). The aluminum current collector has been known to undergo noticeable corrosion in carbonate-based electrolyte solutions containing LiTFSI [26,27]. However, in the case of the SPE containing LiTFSI, no significant corrosion in contact with the passive layer of Al occurred, as shown in Figure 2b, where only a small current (one tenth of that in the Au electrode) flowed at 5 V vs. Li/Li⁺ in the repeated CV measurements. The SPEs tested showed larger stability windows at the Al surface than at the Au surface, and in both cases, the addition of LiPF₆ to LiTFSI was effective to expand the stability window by forming a protective film. Therefore, in the following discussion, the possibility of a

reaction between the SPE and the Al sheet is not considered (although the gradual reaction for a long period may be left uncertain).

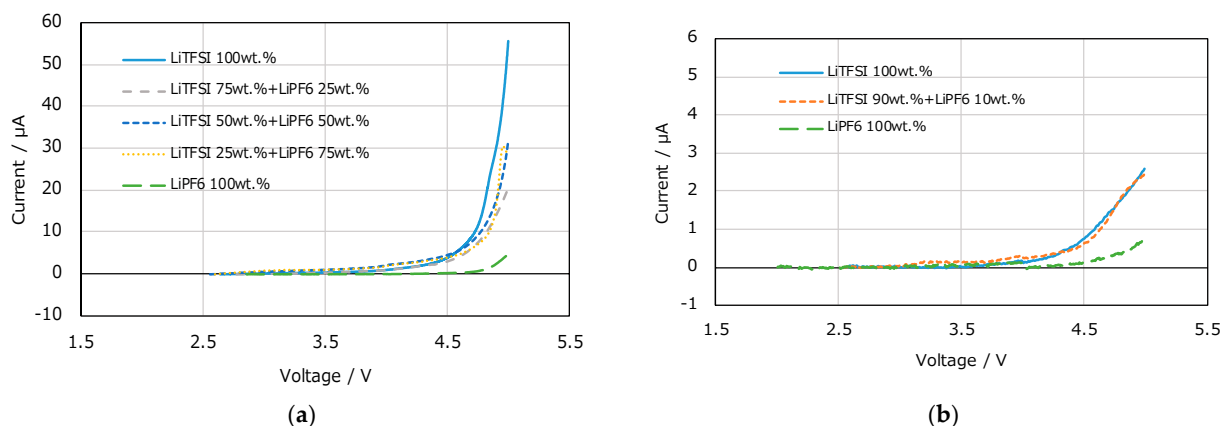


Figure 2. CV curves for (a) Li/PEO-LiTFSI-LiPF₆/Au and (b) Li/PEO-LiTFSI-LiPF₆/Al in the second potential sweep from 2.5 V to 5.0 V vs. Li/Li⁺ at 80 °C.

To clarify the effect of LiPF₆ addition in the PEO-LiTFSI electrolyte, the variation in the interfacial resistance with time between the PEO-LiTFSI-LiPF₆ electrolyte and Li-deintercalated Li_{1-x}CoO₂ at each charged potential was monitored by impedance measurement. A schematic pattern of the impedance measurement combined with constant current–constant voltage charging is shown in Figure 3a. In this example, the cell was charged to 4.2 V vs. Li/Li⁺ at constant current, maintained for 2 h at that voltage by constant voltage, and after being open-circuited, the impedance was measured 20 times. Figure 3b shows an assumed equivalent circuit. The impedance profiles were analyzed to estimate the Li metal/SPE and LCO/SPE resistances using a non-linear instant fit program in the Z view software package (Ver.3.5h).

Figure 3c,d show the time dependence of the impedance spectra for the Li/PEO (LiTFSI 100 wt%)/LiCoO₂ cell and Li/PEO (LiTFSI 80 wt% + LiPF₆ 20 wt%)/LiCoO₂ cell at 4.2 V vs. Li/Li⁺, respectively. The impedance components were separated into the electrolyte bulk resistance (R_b), the electrolyte/Li anode interfacial resistance (R_{Li}), and the electrolyte/LiCoO₂ cathode interfacial resistance (R_{LiCoO_2}) from the high-frequency side. The attribution of (R_{Li}) and (R_{LiCoO_2}) was determined from the resistance values obtained by measuring the impedance of electrodes with different cathode areas. Not all samples measured showed notable changes in resistance (R_b and R_{Li}) with time; however, the time dependence of the resistance at the electrolyte/LiCoO₂ cathode interface (R_{LiCoO_2}) was significantly different between the non-LiPF₆-doped and LiPF₆-doped SPE.

The variations in R_{LiCoO_2} with time for various applied potentials are shown in Figure 4a,b. A large difference was observed in the rate of increase between the systems with and without LiPF₆. As shown in Figure 4a, the PEO-LiTFSI/LiCoO₂ interface resistance R_{LiCoO_2} increased slightly with time, even under the applied voltage of 4.1 V vs. Li/Li⁺, and under higher voltages, the slope increased significantly with time and R_{LiCoO_2} rose exponentially with the applied voltages. The result from the interfacial resistance measurement is consistent with previous reports on the decomposition potential of PEO-related electrolytes, which fell in the range of 3.7–4.1 V [8,9]. In contrast, the interface of PEO-LiTFSI-LiPF₆/LiCoO₂ was largely stabilized by the presence of LiPF₆, as shown in Figure 4b, where the change in resistance with time for the SPEs with LiPF₆ is plotted under applied potentials of 4.2 to 4.4 V vs. Li/Li⁺. At 4.2 V and 4.3 V vs. Li/Li⁺, R_{LiCoO_2} showed almost no variation with time; even at 4.4 V vs. Li/Li⁺, only a slight increase in resistance from 100 Ω to 400 Ω was observed during the exposed time of 50 h, which significantly contrasted with the large increase in resistance from 400 Ω to 20,000 Ω during the 30 h period with the non-doped PEO-LiTFSI system. Therefore, LiPF₆ plays an important role in stabilizing the polymer electrolyte/LiCoO₂ interface, even at only 10 wt% addition.

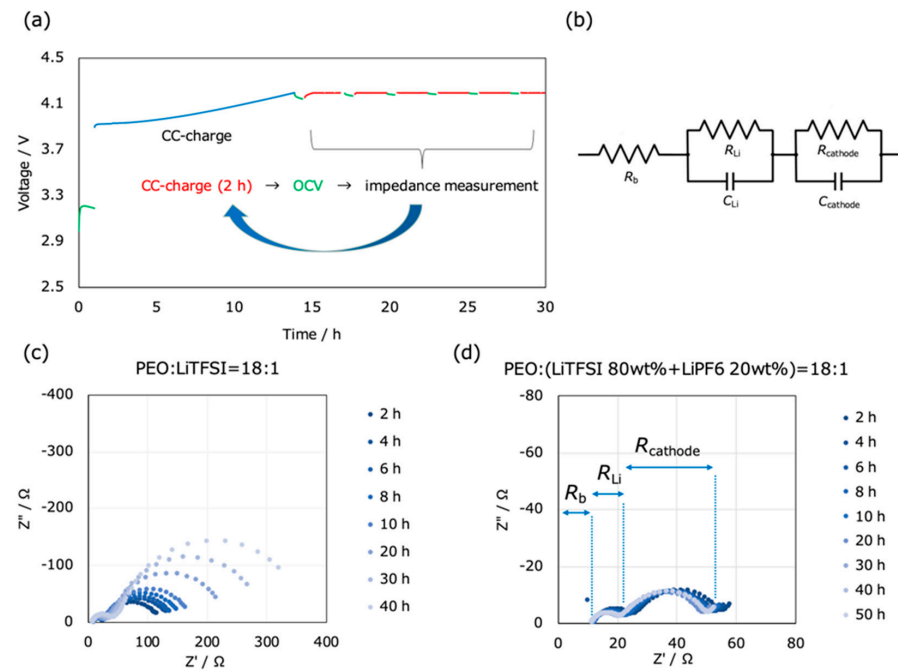


Figure 3. (a) Schematic pattern of the impedance measurement combined with constant current-constant voltage charging. In this example, the cell was charged to 4.2 V vs. Li/Li⁺ by constant current, maintained for 2 h at the voltage (constant voltage charge), and open-circuited, and then, the impedance was measured. The process was repeated 20 times. (b) Assumed equivalent circuit. (c) Time dependence of the impedance spectra for the Li/PEO(LiTFSI 100 wt%)/LiCoO₂ cell at 4.2 V vs. Li/Li⁺. (d) Time dependence of the impedance spectra for the Li/PEO(LiTFSI 80 wt%+LiPF₆ 20 wt%)/LiCoO₂ cell at 4.2 V vs. Li/Li⁺.

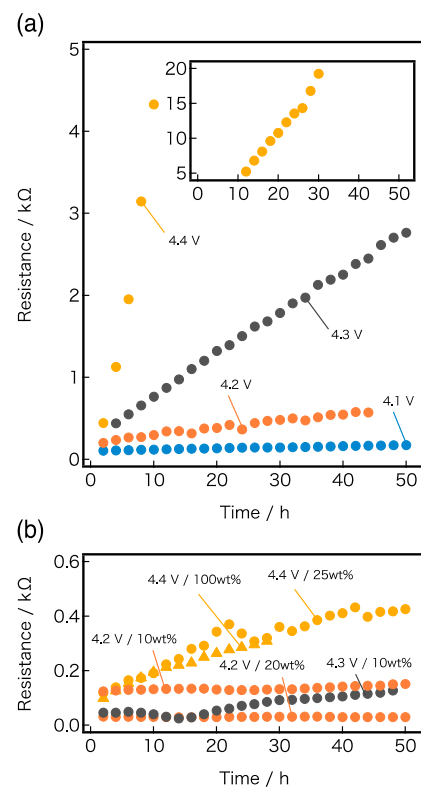


Figure 4. Variation in interfacial resistance, R_{LiCoO_2} , with time under various applied potentials for SPEs (a) without LiPF₆ and (b) with LiPF₆.

Figure 5 shows charge–discharge curves and the cycle performance between 2.5 V and 4.4 V for Li/PEO-LiTFSI-LiPF₆/LiCoO₂ cells with 0 wt%, 25 wt%, and 100 wt% of added LiPF₆. A significant difference in cell performance was observed with and without LiPF₆. The cells with SPE containing LiPF₆ display stable charge/discharge curves and cycling performance with a capacity retention of 150 mAh/g after 20 cycles. The capacity during charge for the cell without LiPF₆ dropped to 100 mAh/g from the first discharge capacity of 170 mAh/g after 20 cycles. In the cut-off voltage of 2.5–4.5 V, degradation of the cycle performance was also appreciably suppressed in the case of LiPF₆ addition (Figure 6). The cell with the SPE containing 10 wt% LiPF₆ maintained a capacity of 100 mAh/g after 100 cycles, the retention of which is 53%, as calculated from the capacity of 190 mAh/g in the first discharge.

The electrochemical stability window of SPE should be the same as that of the electrode potential or higher. For 4 V class cathodes with operating voltages as high as 4.2–4.4 V vs. Li/Li⁺, stability at 4.5 V vs. Li/Li⁺ is, at least, required to compensate for the overpotential during charge [31]. The PEO-based SPE including LiPF₆ as a Li salt has the possibility to meet these criteria, although further electrochemical investigation will be necessary. At the moment, it is unclear as to what the stability enhancement of the polymer/cathode interface can be attributed to by the addition of LiPF₆ as a lithium salt to the PEO electrolyte. Detailed surface analyses are also desirable as a next step.

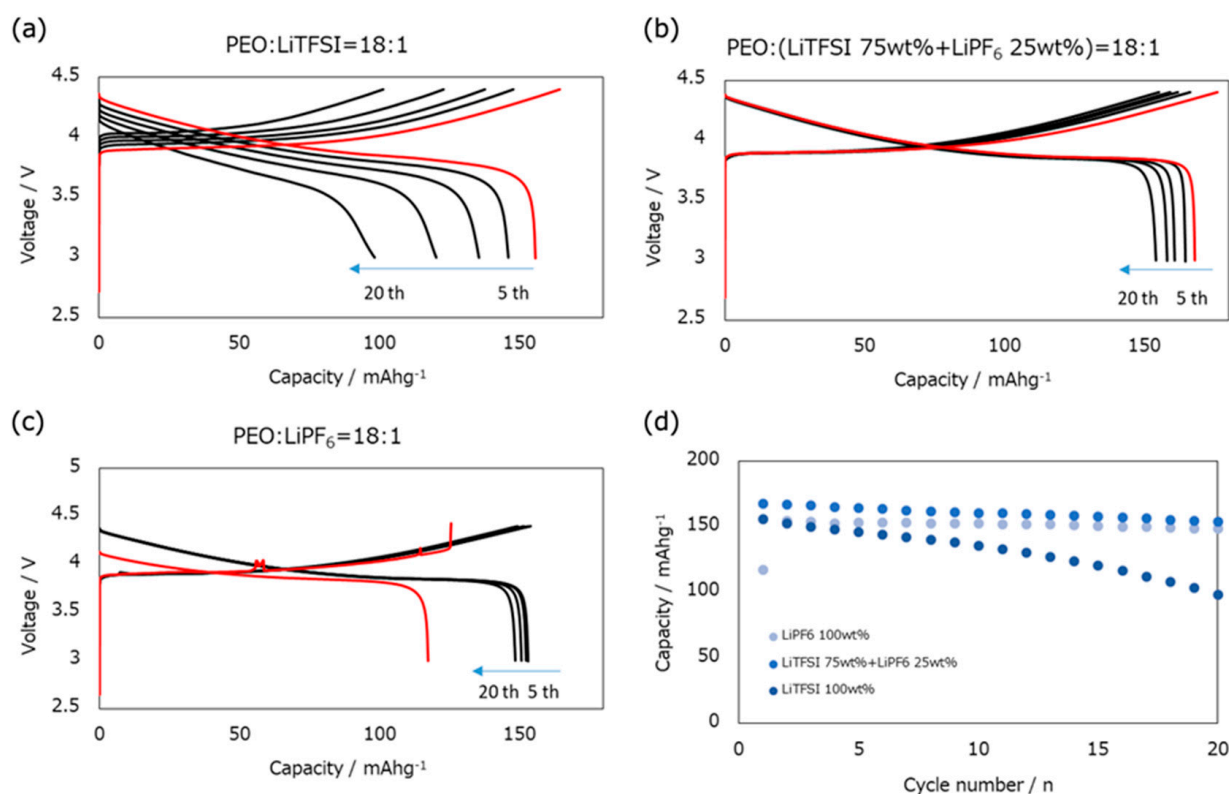


Figure 5. Charge–discharge curves for the Li/PEO-LiTFSI-LiPF₆/LiCoO₂ cells with the addition of (a) 0 wt%, (b) 25 wt%, and (c) 100 wt% LiPF₆, and (d) the cycle performance with cut-off voltages of 2.5 V and 4.4 V with 0.1 C rate at 80 °C. The red lines show the first charge–discharge curves. In the case of PEO:LiPF₆ = 18:1 (c), imperfect penetration of the SPE into the electrode caused a decrease in the first charge capacity because of the low fluent SPE characteristic due to the high concentration of LiPF₆.

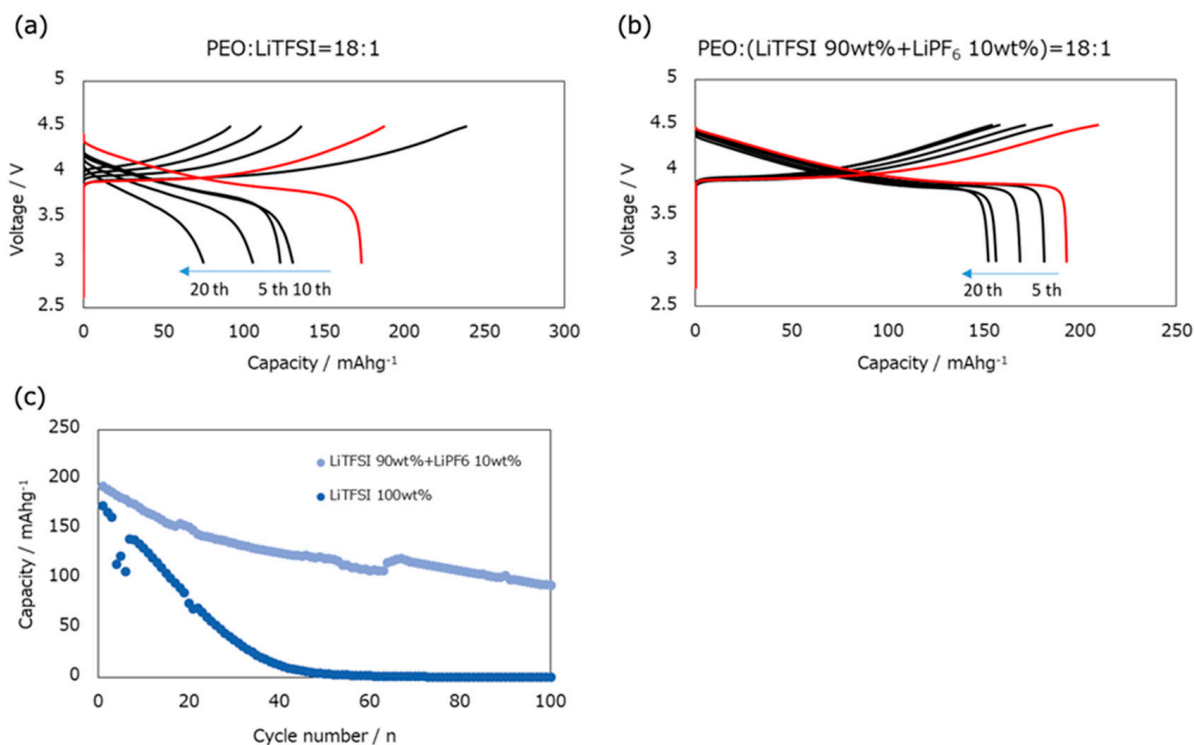


Figure 6. Charge–discharge curves for (a) Li/PEO-LiTFSI/LiCoO₂ and (b) Li/PEO-LiPF₆/LiCoO₂ cells, and (c) the cycle performance. The red lines in (a,b) show the first charge-discharge curves. The cut-off voltage was 2.5–4.5 V with a rate of 0.1 C at 80 °C.

4. Conclusions

The addition of LiPF₆ with LiTFSI (Li(CF₃SO₂)₂N) as lithium salts in a PEO-based electrolyte is effective to stabilize the interface of the SPE and the 4 V class LiCoO₂ cathode material. Impedance measurements of the interface of SPE with LiPF₆ and LiCoO₂ under applied potentials of 4.2–4.4 V vs. Li/Li⁺ revealed that the increase in interface resistance was suppressed at a high potential such as 4.4 V vs. Li/Li⁺. Fairly good cycle performance, even at a cut-off voltage of 4.5 V vs. Li/Li⁺, was obtained from the charge–discharge tests for Li/PEO-Li(CF₃SO₂)₂N-LiPF₆/LiCoO₂ cells. The 10–25 wt% addition of LiPF₆ to LiTFSI was sufficient to trigger an improvement, and this composition had lithium ion conductivity that was almost equal to the non-doped electrolyte. In this report, only an SPE system of PEO with a molecular weight of 600 × 10³ and a typical lithium salt, LiTFSI, was investigated. It is therefore of interest whether the addition of LiPF₆ would have similar effects in polymer electrolytes with different molecular structures from a PEO electrolyte.

Author Contributions: S.T. and Y.T. conceived and designed the experiments. A.T. and K.S. prepared the samples and performed the electrochemical measurements. S.T., D.M., Y.T., O.Y. and N.I. discussed the results and analyzed the data. S.T. and Y.T. wrote the manuscript. All authors have read and agreed to the published version of the manuscript.

Funding: This research received no external funding.

Data Availability Statement: The original contributions presented in the study are included in the article, further inquiries can be directed to the corresponding authors.

Acknowledgments: The authors would like to thank Shinichi Kumakura and Keisuke Nomura of Umicore Japan for extensive discussions and helpful suggestions.

Conflicts of Interest: The authors declare no conflicts of interest.

References

1. Wright, P.V. Electrical conductivity in ionic complexes of poly(ethylene oxide). *Br. Polym. J.* **1975**, *7*, 319–327. [[CrossRef](#)]
2. Armand, M.B.; Choquette, J.M.; Duclot, M. In Extend Abstract. In Proceedings of the 2nd International Meeting on Solid Electrolytes, St. Andrews, UK, 20 September 1978.
3. Gray, P.M. *Solid Polymer Electrolyte*; VHC: Weinheim, Germany, 1991; p. 2.
4. Berthier, C.; Gorecki, W.; Minier, M.; Armand, M.; Chabagno, J.; Rigaud, P. Microscopic investigation of ionic conductivity in alkali metal salts-poly(ethylene oxide) adducts. *Solid State Ionics* **1983**, *11*, 91–95. [[CrossRef](#)]
5. Reiche, A.; Steurich, T.; Sandner, B.; Lobitz, P.; Fleischer, G. Ion transport in gel electrolytes. *Electrochim. Acta* **1995**, *40*, 2153–2157. [[CrossRef](#)]
6. Appetecchi, G.B.; Croce, F.; Mastragostino, M.; Scrosati, B.; Soavi, F.; Zanelli, A. Composite Polymer Electrolytes with Improved Lithium Metal Electrode Interfacial Properties: II. Application in Rechargeable Batteries. *J. Electrochem. Soc.* **1998**, *145*, 4133–4135. [[CrossRef](#)]
7. Fauteux, D.; Massucco, A.; McLin, M.; Van Buren, M.; Shi, J. Lithium polymer electrolyte rechargeable battery. *Electrochimica Acta* **1995**, *40*, 2185–2190. [[CrossRef](#)]
8. Xie, Y.; Tatsumi, K.; Fujieda, T.; Prosini, P.P.; Sakai, T. Solid–State Lithium–Polymer Batteries Using Lithiated MnO₂ Cathodes. *J. Electrochem. Soc.* **2000**, *147*, 2050–2056. [[CrossRef](#)]
9. Appetecchi, G.B.; Croce, F.; Dautzenberg, G.; Mastragostino, M.; Ronci, F.; Scrosati, B.; Soavi, F.; Zanelli, A.; Alessandrini, F.; Prosini, P.P. Composite Polymer Electrolytes with Improved Lithium Metal Electrode Interfacial Properties: I. Electrochemical Properties of Dry PEO–LiX Systems. *J. Electrochem. Soc.* **1998**, *145*, 4126–4132. [[CrossRef](#)]
10. Osaka, T.; Homma, T.; Momma, T.; Yarimura, H. In situ observation of lithium deposition processes in solid polymer and gel electrolytes. *J. Electroanal. Chem.* **1997**, *421*, 153–156. [[CrossRef](#)]
11. Brissot, C.; Rosso, M.; Chazalviel, J.-N.; Lascaud, S. Dendritic growth mechanisms in lithium/polymer cells. *J. Power Sources* **1999**, *81–82*, 925–929. [[CrossRef](#)]
12. Liu, S.; Wang, H.; Imanishi, N.; Zhang, T.; Hirano, A.; Yamamoto, O.; Yang, J.; Takeda, Y. Effect of co-doping nano-silica filler and N-methyl-N-propylpiperidinium bis(trifluoromethanesulfonyl)imide into polymer electrolyte on Li dendrite formation in Li/poly(ethylene oxide)-Li(CF₃SO₂)₂N/Li. *J. Power Sources* **2011**, *196*, 7681–7686. [[CrossRef](#)]
13. Imanishi, N.; Ono, Y.; Hanai, K.; Uchiyama, R.; Liu, Y.; Hirano, A.; Takeda, Y.; Yamamoto, O. Surface-modified meso-carbon microbeads anode for dry polymer lithium-ion batteries. *J. Power Sources* **2008**, *178*, 744–750. [[CrossRef](#)]
14. Kawakubo, M.; Takeda, Y.; Yamamoto, O.; Imanishi, N. High capacity carbon anode for dry polymer lithium-ion batteries. *J. Power Sources* **2013**, *225*, 187–191. [[CrossRef](#)]
15. Fergus, J.W. Ceramic and polymeric solid electrolytes for lithium-ion batteries. *J. Power Sources* **2010**, *195*, 4554–4569. [[CrossRef](#)]
16. Kim, J.G.; Son, B.; Mukherjee, S.; Schuppert, N.; Bates, A.; Kwon, O.; Choi, M.J.; Chung, H.Y.; Park, S. A review of lithium and non-lithium based solid state batteries. *J. Power Sources* **2015**, *282*, 299–322. [[CrossRef](#)]
17. Mindemark, J.; Lacey, M.J.; Bowden, T.; Brandell, D. Beyond PEO—Alternative host materials for Li⁺-conducting solid polymer electrolytes. *Prog. Polym. Sci.* **2018**, *81*, 114–143. [[CrossRef](#)]
18. Strauss, E.; Menkin, S.; Golodnitsky, D. On the way to high-conductivity single lithium-ion conductors. *J. Solid State Electrochem.* **2017**, *21*, 1879–1905. [[CrossRef](#)]
19. Jung, Y.-C.; Park, M.-S.; Kim, D.-H.; Ue, M.; Eftekhari, A.; Kim, D.-W. Room-Temperature Performance of Poly(Ethylene Ether Carbonate)-Based Solid Polymer Electrolytes for All Solid State Lithium Batteries. *Sci. Rep.* **2017**, *7*, 17482. [[CrossRef](#)]
20. Li, Z.; Li, A.; Zhang, H.; Lin, R.; Jin, T.; Cheng, Q.; Xiao, X.; Lee, W.K.; Ge, M.; Zhang, H.; et al. Interfacial engineering for stabilizing polymer electrolytes with 4 V cathodes in lithium metal batteries at elevated temperature. *Nano Energy* **2020**, *72*, 104655. [[CrossRef](#)]
21. Li, Q.; Takeda, Y.; Imanishi, N.; Yang, J.; Sun, H.Y.; Yamamoto, O. Cycling performances and interfacial properties of a Li/PEO–Li(CF₃SO₂)₂N–ceramic filler/LiNi_{0.8}Co_{0.2}O₂ cell. *J. Power Sources* **2001**, *97–98*, 795–797. [[CrossRef](#)]
22. Aihara, Y.; Kuratomi, J.; Bando, T.; Iguchi, T.; Yoshida, H.; Ono, T.; Kuwana, K. Investigation on solvent-free solid polymer electrolytes for advanced lithium batteries and their performance. *J. Power Sources* **2003**, *114*, 96–104. [[CrossRef](#)]
23. Kobayashi, Y.; Seki, S.; Yamanaka, A.; Miyashiro, H.; Mita, Y.; Iwahori, T. Development of high-voltage and high-capacity all-solid-state lithium secondary batteries. *J. Power Sources* **2005**, *146*, 719–722. [[CrossRef](#)]
24. Seki, S.; Kobayashi, Y.; Miyashiro, H.; Mita, Y.; Iwahori, T. Fabrication of High-Voltage, High-Capacity All-Solid-State Lithium Polymer Secondary Batteries by Application of the Polymer Electrolyte/Inorganic Electrolyte Composite Concept. *Chem. Mater.* **2005**, *17*, 2041–2045. [[CrossRef](#)]
25. Li, Q.; Imanishi, N.; Hirano, A.; Takeda, Y.; Yamamoto, O. Four volts class solid lithium polymer batteries with a composite polymer electrolyte. *J. Power Sources* **2002**, *110*, 38–45. [[CrossRef](#)]
26. Yang, H.; Kwon, K.; Devine, T.M.; Evans, J.W. Aluminum Corrosion in Lithium Batteries An Investigation Using the Electrochemical Quartz Crystal Microbalance. *J. Electrochem. Soc.* **2000**, *147*, 4399–4407. [[CrossRef](#)]
27. Morita, M.; Shibata, T.; Yoshimoto, N.; Ishikawa, M. Anodic behavior of aluminum in organic solutions with different electrolytic salts for lithium ion batteries. *Electrochimica Acta* **2002**, *47*, 2787–2793. [[CrossRef](#)]
28. Vallée, A.; Besner, S.; Prud'homme, J. Comparative study of poly(ethylene oxide) electrolytes made with LiN(CF₃SO₂)₂, LiCF₃SO₃ and LiClO₄: Thermal properties and conductivity behavior. *Electrochim. Acta* **1992**, *37*, 1579–1583. [[CrossRef](#)]

29. Lascaud, S.; Perrier, M.; Vallee, A.; Besner, S.; Prud'Homme, J.; Armand, M. Phase Diagrams and Conductivity Behavior of Poly(ethylene oxide)-Molten Salt Rubbery Electrolytes. *Macromolecules* **1994**, *27*, 7469–7477. [[CrossRef](#)]
30. Labrèche, C.; Lévesque, I.; Prud'homme, J. An Appraisal of Tetraethylsulfamide as Plasticizer for Poly(ethylene oxide)–LiN(CF₃SO₂)₂ Rubbery Electrolytes. *Macromolecules* **1996**, *29*, 7795–7801. [[CrossRef](#)]
31. Dias, F.B.; Plomp, L.; Veldhuis, J.B. Trends in polymer electrolytes for secondary lithium batteries. *J. Power Sources* **2000**, *88*, 169–191. [[CrossRef](#)]

Disclaimer/Publisher's Note: The statements, opinions and data contained in all publications are solely those of the individual author(s) and contributor(s) and not of MDPI and/or the editor(s). MDPI and/or the editor(s) disclaim responsibility for any injury to people or property resulting from any ideas, methods, instructions or products referred to in the content.